Article

Discovery Medicine 2026; 38(205): 505–519
https://doi.org/10.24976/Discov.Med.202638205.42

Capsaicin Improves Fatty Acid Oxidation in Skeletal Muscle Cells Through the TRPV1/TFEB-Dependent Lipophagy Enhancement

Lijuan Wang[1,†], Yihua Zhang[2,†], Shuyun Wang[3], Li Li[1], Yingru Hu[1], Ying Chang[3], Zhidan Luo[3,*]

[1]Department of Hypertension and Endocrinology, Center for Hypertension and Metabolic Diseases, Daping Hospital, Army Medical University, Chongqing Institute of Hypertension, 400042 Chongqing, China
[2]Department of Cardiology, Fifth People's Hospital of Chongqing, Renji Hospital of Chongqing University, 400062 Chongqing, China
[3]Department of Geriatric Medicine, Chongqing Clinical Research Center for Geriatric Diseases, Chongqing General Hospital, Chongqing University, 400013 Chongqing, China
*Correspondence: zhidanluo@126.com (Zhidan Luo)
[†]These authors contributed equally.
Submitted: 29 September 2025 Revised: 15 December 2025 Accepted: 7 January 2026 Published: 20 February 2026

Background: Excess intramyocellular lipid induces lipotoxicity, which has been implicated in the development of insulin resistance and metabolic diseases. Although dietary capsaicin has been shown to reduce intramyocellular lipid content in mice, the underlying mechanisms remain unclear. This study aims to investigate the effects of capsaicin on lipophagy and fatty acid metabolism in skeletal muscle cells and explore the underlying mechanisms.

Methods: Wild-type and transient receptor potential vanilloid channel 1 (*TRPV1*) knock-out (KO) mice were fed a high-fat diet (HD) with or without capsaicin for 4 months. They underwent a fasting exercise to induce autophagy before measurement. C2C12 myotubes were cultured with palmitate and treated with or without capsaicin, specific antagonists, or transcription factor EB (TFEB) RNAi. Respiratory exchange ratio (RER), metabolic parameters and muscle mitochondrial fatty acid oxidation were assessed. Autophagic flux was detected using the Premo Autophagy Tandem Sensor. TFEB transcriptional activity was detected by luciferase assays. RNA-sequencing, Western blotting, and immunofluorescence were conducted to analyze the expression of lipophagy-related genes.

Results: Lipid overload inhibited fatty acid oxidation and impaired autophagy flux in muscles of HD-fed wild-type mice and myotubes cultured with palmitate. Although capsaicin significantly attenuated this inhibition ($p < 0.05$), the effect was not replicated in the TRPV1 KO mice ($p > 0.05$). In cultured myotubes, capsaicin dose-dependently promoted the expression of TFEB and also enhanced TFEB transcriptional activity ($p < 0.05$). This led to increased acidic lysosomes, degradation of p62 and perilipin 2, and improved fatty acid oxidation ($p < 0.05$). The TRPV1 antagonist, the calcineurin inhibitor, or TFEB siRNA significantly inhibited the effects of capsaicin ($p < 0.05$).

Conclusions: Capsaicin ameliorates impaired lipophagy and fatty acid oxidation in lipid-overloaded skeletal muscle cells through a TRPV1/TFEB-dependent pathway.

Keywords: capsaicin; lipophagy; skeletal muscle; TRPV1; TFEB; fatty acid oxidation

Introduction

Excessive lipid accumulation in skeletal muscle cells is a key factor in the development of insulin resistance [1]. Lipid autophagy, also called lipophagy, has been identified in lipolysis mediated by acid lipases in lysosomes [2]. The impairment of Lysosomal acidification and autophagic flux has also been shown to contribute to lipotoxicity in obesity-related diseases [3–5]. Transcription factor EB (TFEB)-mediated lysosome activation protects against the impairment of obesity or high-fat diet in the kidney [3] and adipose tissues [6]. Previous study has also posited that the inhibition of autophagy by bafilomycin exaggerates the lipid accumulation in L6 myotubes, which can be restored by the autophagy agonist rapamycin [7]. Thus, safe and effective autophagy-regulating approaches may help to prevent lipotoxicity and related metabolic diseases.

Capsaicin, the primary active component in chili peppers, acts as an agonist for the transient receptor potential vanilloid channel 1 (TRPV1). TRPV1 is expressed in nerves and numerous metabolically active tissues, making it a promising target for metabolic regulation [8,9]. Dietary capsaicin has been demonstrated in rodents or humans to attenuate metabolic disorders, including obesity,

diabetes, dyslipidemia, fatty liver, and hypertension [10–12]. A recent meta-analysis of randomized controlled trials showed that capsaicin, capsinoids, and pepper-based products significantly reduce total cholesterol and triglyceride levels in overweight or obese individuals, especially when used at higher doses ($\geq$10 mg) and for extended durations ($\geq$12 weeks) [13]. Animal and cellular studies indicate that capsaicin probably regulates lipid metabolism through distinct mechanisms in various cell types. A study on macrophages suggested that capsaicin modulated cholesterol uptake and efflux through the TRPV1/Peroxisome proliferator-activated receptor (PPAR) γ pathway [14]. Another study on HepG2 cells demonstrated that capsaicin reduced lipid accumulation by activating mitophagy [15]. Additionally, a study on mice and cell models of Alzheimer's disease revealed that capsaicin enhanced lysosomal function through PPARα, thereby reducing hippocampal lipid deposition and improving cognitive function [16].

Functional TRPV1 expression has been identified in primary human and rodent myotubes, along with L6 and C2C12 cell lines [17,18]. This channel is functionally significant in regulating myotube differentiation, muscle quality, and exercise performance [17,19,20]. Consistently, Abdillah *et al*. [21] reported that dietary capsaicin promotes thermogenesis, myotube differentiation, and lipid metabolism in rat skeletal muscle cells. Our earlier study also found that a 0.01% dietary capsaicin supplementation for 4 months significantly reduced high-fat diet-induced lipid accumulation in mouse skeletal muscle, while improving insulin resistance and exercise endurance [17]. However, the specific mechanisms, including any role of lipophagy, remain unclear. Thus, the objective of this study was to examine the impact of capsaicin on lipophagy and fatty acid metabolism in skeletal muscle cells and its related mechanisms.

Materials and Methods

Animal Care

The C57BL/6J wild-type (WT) mice and TRPV1 knockout (KO) mice were sourced from Jackson Laboratory (Bar Harbor, ME, USA) and bred in-house. Fifteen male mice of each strain, aged 6–8 weeks, were randomly assigned to the following 3 groups: ND (normal diet), HD (high-fat diet with 60% Kcal from fat), and HC (HD with 0.01% capsaicin supplementation), with 5 mice in each group. Numerous studies, from our team [17,22] and others [16,23], have established that a 4-month intervention with a high-fat diet containing 0.01% capsaicin attenuates metabolic disorders in mice without affecting their food consumption. Therefore, we adopted a similar capsaicin-supplemented dietary regimen. Diets were acquired from Chongqing Tengxin Inc. (Chongqing, China). Capsaicin ($\geq$95% purity, M2028) was purchased from Sigma-Aldrich and used to produce the HC diet by Tengxin Inc. Mice were maintained on a 12-h light/dark cycle with free access to rodent chow and water. Body weight and daily food intake were measured and recorded monthly. Mice were maintained on their respective dietary regimens for a 4-month period prior to sacrifice. Ethical approval for the study protocol was obtained on March 15, 2017. All mice were cared for and used in the study in compliance with international, national, and institutional guidelines, following approval from our Institutional Animal Care and Research Advisory Committee.

Fasting Exercise and Respiratory Exchange Ratio Measurement

The exercise protocol and respiratory exchange ratio (RER) measurement were carried out following the methods from our previous studies [17,24]. All mice underwent a period of acclimation to the treadmill (XR-PT-10B, Xinruan Technology Co., Ltd., Shanghai, China) 2 days before fasting exercise and sacrifice. On the first day, the mice were placed on the treadmill for a 5-minute run at 7 m/min and a 10-minute run at 10 m/min. On the second day, the mice underwent a 30-minute run at 10 m/min. On the third day, after fasting for 14 hours, the mice were subjected to a 40-minute run at 10 m/min to induce energy stress and autophagy. After fasting exercise, the O_2 expenditure and CO_2 generation of mice were immediately detected using the comprehensive laboratory animal monitoring system (Columbus, OH, USA). RER was calculated as the ratio of CO_2 production to O_2 consumption. Due to agitation during RER measurements, one mouse in each group was excluded for RER analysis.

Blood Analysis

After fasting exercise, the mice were anesthetized by intraperitoneal administration of a ketamine/xylazine mixture (ketamine 100 mg/kg, xylazine 10 mg/kg) in saline. Blood samples obtained from the carotid arteries, and mice were euthanized by exsanguination, and skeletal muscles (gastrocnemius and soleus) were isolated and cryopreserved. Serum concentrations of triglycerides, cholesterol, and lactic acid were quantified within 24 hours using commercial assay kits (E1003, E1021 and E2063) from Applygen Technologies Inc. (Beijing, China).

Muscle Triglycerides and Glycogen Measurements

Colorimetric assays were employed to measure muscle glycogen and triglyceride stores according to the provided protocols. Briefly, the gastrocnemius muscles were homogenized in 5% NP-40 for triglyceride detection. Then, for total lipid extraction, muscle tissues were subjected to multiple rounds of heating and cooling. Finally, muscle triglycerides were assayed according to the procedure detailed in the kit (ab65336; Abcam, MA, USA). For glycogen quantification, gastrocnemius muscles were homog-

enized in distilled water (5 mg tissue per 100 µL), centrifuged at 1800 RPM for 10 minutes, and the resulting supernatant was analyzed following the kit's (ab65620; Abcam, CA, USA) protocol.

Muscle Mitochondrial Isolation

Functionally intact mitochondria were isolated from the gastrocnemius muscle using a commercial kit (C3606, Beyotime, Shanghai, China). Briefly, tissue was homogenized on ice in a Mitochondria Isolation Buffer (210 mM Sucrose, 2 mM EGTA, 40 mM NaCl, 30 mM HEPES, pH 7.4) with a glass Dounce homogenizer and a high-speed drill. The homogenate was sequentially centrifuged at low speed (900 ×g, 10 min, 4 °C) and then high speed (10,000 ×g, 10 min, 4 °C) to isolate mitochondria. The resulting mitochondrial pellet was resuspended in fatty acid oxidation media to assess the oxidation rate. The quality of mitochondria was confirmed by the pronounced increase in oxygen consumption rate after ADP and succinate addition, measured using an Oxygraph-2k system (Oroboros, Innsbruck, Austria) according to our established laboratory protocol [24].

Fluorescence Co-Staining for Myosin Heavy Chain (MyHC), TFEB and TRPV1

Gastrocnemius muscles cross-sections were cut at –20 ℃ with a cryostat microtome (Leica Biosystems, Wetzlar, Germany). Air-dried sections were fixed in 4% PFA (20 min), blocked (30 min), and incubated with primary antibodies against the slow fiber MyHC, MyH7 (1:200; AF7533; Beyotime, Shanghai, China), or TFEB (1:200; PA5-96632; Thermo Fisher Scientific, MA, USA) and against TRPV1 (1:200; 75-254; Thermo Fisher Scientific, MA, USA) for 1 hour at 37 °C. Subsequent to three washes, slides were incubated with fluorescently labeled secondary antibodies (31569 and T-2769; Thermo Fisher Scientific, MA, USA; 1:1000; 30 min, 37 °C, dark). After further washing, they were mounted using ProLong Gold antifade reagent with DAPI (P36941, Thermo Fisher Scientific, MA, USA), followed by imaging. Images were taken by fluorescence microscopy (TE2000, Nikon, Tokyo, Japan).

RNA-Sequencing and Data Analysis

RNA extraction and the whole transcriptome RNA-sequencing were performed by Knorigene Technologies (Chongqing, China). SE50 sequencing yielded at least 10 million clean reads per sample. Raw sequencing data have been uploaded to NCBI SRA (PRJNA1290807). Differential gene expression levels were assessed using FPKM values by calculating the Log2 fold-change of ND and HC samples relative to the HD group. A Log2 fold-change threshold was arbitrarily set to define significant differential expression.

Quantitative Reverse-Transcribed Polymerase Chain Reaction (qRT-PCR)

We performed total RNA extraction from frozen soleus muscles with TRIzol reagent (15596-026; Invitrogen, CA, USA). RNA quality was assessed on a NanoDrop 1000 spectrophotometer (Thermo Scientific, MA, USA). Subsequent cDNA synthesis was performed on 2 µg of RNA employing a commercial kit (#04896866001; Roche, Basel, Switzerland). qPCR reactions were set up with 2 µL of cDNA and SYBR Premix Ex Taq II (Bio-Rad, CA, USA) in a LightCycler 96 instrument (Roche, Basel, Switzerland), using a thermal profile comprising 95 °C for 30 s, then 40 cycles of 95 °C for 5 s and 60 °C for 30 s. Primer sequences are provided in **Supplementary Table 1**. Data analysis was conducted with the instrument's software (LightCycler 96, v1.1, Roche Diagnostics, Mannheim, Germany). Relative mRNA expression levels were calculated using the comparative threshold cycle ($\Delta\Delta$Ct) method. Briefly, the Ct values of target genes were first normalized to the geometric mean of Ct values from reference genes within the same sample to obtain ΔCt values. The ΔCt of the experimental group was then normalized to the mean ΔCt of the control group to yield $\Delta\Delta$Ct. The relative mRNA expression was expressed as $2^{-\Delta\Delta Ct}$ and finally normalized as the fold change of the ND group.

Cell Culture

Mouse C2C12 myoblasts (RRID: CVCL_0188; Shanghai Institute for Biological Sciences, Shanghai, China) were maintained in Dulbecco's modified Eagle's medium (DMEM; Gibco, NY, USA) with 10% fetal bovine serum (FBS; Gibco, NY, USA) at 37 °C in a humidified atmosphere of 5% CO_2 and 95% O_2. The switch to differentiation medium (DMEM with 2% horse serum, Gibco) was performed at 80% myoblast confluence. After 4 days, the myoblasts were differentiated into myotubes and used in the subsequent experiments. The C2C12 cell line was authenticated by Short tandem repeat (STR) profiling upon receipt and tested for mycoplasma contamination prior to experimentation.

Cell Treatment

A 10 mM palmitate stock solution combined with 10% bovine serum albumin (BSA; A8806, Sigma-Aldrich, MO, USA) was prepared according to the published method [22] with minor modifications. 27.84 mg sodium palmitate (P9767, Sigma-Aldrich, MO, USA) was dissolved in 1 mL ethanol at 55 °C and diluted in 9 mL DMEM with 11% fatty acid-free BSA (BAH66; Equitech-bio inc., TX, USA) at 45–50 °C. The control stock solution with only ethanol and BSA was prepared according to the same procedure except for the palmitate addition. The stock solutions were pre-warmed at 37 °C before use. Myotubes were treated with 0.5 mM palmitate (0.5% BSA) in DMEM for 20 hours to induce lipid accumulation and insulin resistance

as described previously [22,25]. Myotubes were treated with different concentrations (0.1 uM, 1 uM and 10 uM) of capsaicin to explore the dose-dependent effect on lipid content and TFEB expression. Myotubes were also treated with various combinations of palmitate (PA, 0.5 mM), capsaicin (CAPS, 1 μM), capsazepine (CAPZ, 10 μM), EGTA-AM (300 μM), cyclosporine A (CsA, 200 μM), and chloroquine (CQ, 50 μM) as established in prior published experiments for 20 hours. Capsaicin (≥98% purity, 211275), capsazepine (≥98% purity, C191), EGTA-AM (324628), cyclosporine (≥95% purity, SML1018), and chloroquine (C6628) were all purchased from Sigma-Aldrich. Then, myotubes were washed and starved in Earle's balanced salt solution (EBSS; C0213; Beyotime, Shanghai, China) for 4 hours to induce autophagy before assays.

Oil Red O Staining

Cells were sequentially processed for lipid staining by rinsing with ice-cold PBS, fixing with 4% PFA (10 min, RT), and incubating with a freshly prepared, filtered 60% Oil Red O working solution (from a stock of 500 mg/100 mL isopropanol; #00625, Sigma-Aldrich) for 15 min, followed by PBS rinses and light microscopic observation.

Measurement of Fatty Acid Uptake and Oxidation

C2C12 myotubes were cultured in a 96-well CellBIND® microplate and pre-treated for 20 hours with CQ, or capsaicin in the presence or absence of capsazepine (CAPZ). Then, the cells were washed with PBS before use. Fatty acid uptake and oxidation were measured according to the published methods with minor modifications [26,27]. Cultured cells or freshly isolated muscle mitochondria were incubated in 100 μL fatty acid oxidation media containing 0.3% BSA, 0.1 mM palmitate, 0.4 μCi/mL 14C-palmitate (PerkinElmer), and 1 mM carnitine (Sigma-Aldrich). A 96-well UniFilter® microplate, soaked with NaOH (1 M), was mounted on top of the CellBIND® plate to trap the CO_2 produced. After 3 hours' incubation at 37 °C, 50 μL perchloric acid (1M) was added to the media to stop the reaction and liberate the CO_2. After one additional hour at room temperature, the captured CO_2 in the UniFilter® microplate was used for radioactivity assay. The cells in the CellBIND® microplate were washed with cold PBS and used to assess cell-associated (CA) radioactivity with a PerkinElmer scintillation counter. We determined the protein content in each well. The sum of 14C-labeled CO_2 and CA was considered as the total fatty acid uptake. The rate of fatty acid complete oxidation was calculated as $CO_2/(CO_2 + CA)$.

Detection of Autophagic Flux

The autophagic flux in C2C12 cells was detected using the Premo Autophagy Tandem Sensor RFP-GFP-LC3B Kit (P36239; Thermo Fisher Scientific, MA, USA) according to the manufacturer's instructions. 24 hours after the RFP-GFP-LC3B transfection, C2C12 cells were treated with combinations of PA (0.5 mM), CAPS (1 μM), and CAPZ (10 μM) for 20 hours. Then, cells were washed and starved for 4 hours in EBSS. Fluorescent images were taken using fluorescence microscopy (TE2000, Nikon, Tokyo, Japan) and quantified using the Fiji software. Quantification of autophagic flux per cell was based on the ratio of RFP puncta to total signal puncta in the merged image.

Determination of Acidic Lysosome Contents

C2C12 Cells were rapidly washed twice with DMEM, incubated with 2 μg/mL Hoechst 33342 (C1022, Beyotime, Shanghai, China) at 37 °C for 5 min, and then rapidly washed twice again with DMEM. Next, they were incubated with 50 nM LysoTracker Green DND-26 (L7526; Thermo Fisher, Scientific, MA, USA) at 37 °C for 2 min, followed by two rapid washes with DMEM before imaging under a microscope (TE2000, Nikon, Japan). Mean fluorescence intensity was calculated using Fiji software to quantify the lysosomal content.

Transmission Electron Microscope Observation

For TEM analysis, fresh soleus muscle cubes and harvested C2C12 myotubes were fixed in 2% glutaraldehyde (4 °C, overnight), post-fixed in 1% OsO_4, dehydrated in ethanol, and embedded in epoxy resin. Following staining with uranyl acetate and lead citrate, ultrathin (60 nm) sections on copper grids were visualized using a Hitachi H-7100 microscope.

Other Methods

Imaging TFEB cellular localization, fluorescence co-staining for LDs and lysosomal-associated membrane protein 1 (LAMP1), dual-luciferase reporter assay, calcineurin activity assay, TFEB siRNA knockdown, Western blotting, and co-immunoprecipitation (Co-IP) were performed according to standard protocols, as detailed in **Supplementary Material 1**.

Statistical Analysis

Data were presented as the means ± standard error of the means (SEM) with at least three independent experiments. Statistical analyses were conducted in GraphPad Prism 10 (GraphPad Software, Inc., CA, USA), using unpaired Student's *t*-tests or one-way ANOVA with Bonferroni post-hoc tests, where appropriate. A two-tailed *p*-value of less than 0.05 defined statistical significance.

Results

Dietary Capsaicin Improves Fat Oxidation After Fasting Exercise in High-Fat Diet-Fed Mice

Despite the absence of differences in the amount of food intake between the evaluated groups ($p > 0.05$) (Fig. 1A), weight gain induced by a high-fat diet (HD) was

reduced significantly by capsaicin supplementation in wild-type (WT) mice ($p < 0.05$), but not in *TRPV1* gene knockout (KO) mice ($p > 0.05$) (Fig. 1B). Compared with WT mice fed with a normal diet (ND), the respiratory exchange ratio (RER) at rest was lower in mice fed with HD ($p < 0.05$) (**Supplementary Fig. 1**). It suggested that long- Immediately after 40 minutes of running under fasted conditions, mice were measured for RER. They were then euthanized for blood collection and biochemical analysis. Due to agitation during RER measurements, one mouse in each group was excluded for RER analysis. term HD led to greater fat utilization at rest. Interestingly, after 40 minutes of fasting exercise, the RER was significantly higher in HD-fed WT mice ($p < 0.05$) (Fig. 1C). It indicated that, although there's an energetic adaptation to greater fat utilization at rest, the fat oxidation ability under energy stress was impaired in long-term HD-fed mice. Consistently, the fasting plasma triglyceride (Fig. 1D) and lactic acid (Fig. 1E) were significantly higher in WT mice on HD compared with the normal diet (ND) ($p < 0.05$). Fortunately, the HD-induced changes of RER, plasma triglyceride, and lactic acid under energy stress were significantly attenuated by dietary capsaicin in WT mice ($p < 0.05$), but the effects were not observed in TRPV1 KO mice ($p > 0.05$) (Fig. 1C–E). Neither HD nor capsaicin supplementation affected the plasma cholesterol level after fasting exercise (Fig. 1F). It implies that capsaicin may improve fatty acid utilization after fasting exercise in HD-fed mice through the TRPV1 signaling pathway.

Dietary Capsaicin Attenuates the HD-Induced Inhibition of the Mitochondrial Palmitate Oxidation and the mRNA Expression Related to Autophagy and Fatty Acid Metabolism

It is known that fuel utilization and switching can be affected by energy substrate contents in muscles. Thus, we isolated the gastrocnemius muscles of mice 4 hours after the 40-minute fasting exercise. The triglyceride content was higher ($p < 0.05$) (Fig. 2A), while the glycogen content was lower ($p < 0.05$) (Fig. 2B) in HD-fed mice. Then, we detected the 14-C-palmitate oxidation in incubated mitochondria isolated freshly. The method used for mitochondria isolation was validated by immunoblotting and respiratory function assays. The isolated fraction was enriched with the mitochondrial marker, free of nuclear contamination, and potentially contained only minimal cytoplasmic traces (**Supplementary Fig. 2**). The functional capacity was confirmed by the pronounced increase in oxygen consumption rate after the addition of ADP and succinate, the substrates for mitochondrial respiratory Complex I and Complex II (**Supplementary Fig. 3**). It was shown that the palmitate oxidation rate was significantly inhibited by HD in both WT and KO mice ($p < 0.05$) (Fig. 2C,D). Dietary capsaicin supplements remarkably restored fatty acid oxidation in WT mice ($p < 0.05$) but not in KO mice ($p > 0.05$) (Fig. 2C,D). To further reveal the changes in transcriptome profile, we isolated total cellular RNAs from the soleus muscles of WT groups for transcriptome sequencing (RNA-Seq). The heat map illustrated RNA-Seq differential expression related to autophagy (Fig. 2E) and fatty acid metabolism (Fig. 2F). Autophagy-related differential expression levels were verified by qRT-PCR. Compared with the ND group, the mRNA expression levels of MAP1LC3B, TFEB, Sqstm1, and LAMP1 were all inhibited in the HD group of mice ($p < 0.05$), which were significantly restored in the HC group of WT mice ($p < 0.05$), rather than in KO mice ($p > 0.05$) (Fig. 2G,H). These results suggest that capsaicin may counteract the damage of HD on mitochondrial palmitate oxidation and autophagy through the TRPV1 signaling pathway.

Dietary Capsaicin Promotes Lipid Clearance via Lysosomal Activation in Skeletal Muscle

We further detected the distribution of TRPV1 in mouse gastrocnemius muscles, which contain different types of muscle fibers. Representative immunofluorescence staining showed that TRPV1 (green) mainly existed on the membrane of most muscle fibers in the gastrocnemius and was also expressed within the cytoplasm of type I fibers labeled with anti-MyHC (red) (Fig. 3A). Type I fibers contain more lipids and mitochondria than type II fibers and principally rely on oxidative phosphorylation for ATP production. Immunofluorescence staining also showed that TRPV1 (green) and TFEB (red) co-existed in the cytoplasm of a subset of muscle fibers. Therefore, for our experimental samples, we selected muscle tissues like gastrocnemius, which contain a mixture of various fiber types.. Given the potential role of TRPV1 in lipid oxidation and autophagy, lipid droplets and the lysosomal marker, LAMP1, were co-stained by immunofluorescence in the gastrocnemius muscles of mice 4 hours after a 40-minute run in the fasted state. It was shown that HD led to more intramyocellular lipid accumulation and less LAMP1 expression ($p < 0.05$). These effects were attenuated by dietary capsaicin supplementation ($p < 0.05$) (Fig. 3B).

Then, we detected the protein expression of the key genes involved in autophagy and lipid droplet coating in WT skeletal muscles. It was shown that HD led to remarkably decreased TFEB ($p < 0.05$) and LAMP1 ($p < 0.05$) but increased P62 ($p < 0.05$) and Perilipin 2 (PLIN2) ($p < 0.05$) protein levels, and these changes were significantly attenuated by dietary capsaicin ($p < 0.05$) (Fig. 3C). The LC3B-II/I ratio showed a mild upward trend in the HD group, but no significant differences ($p > 0.05$) were observed among all groups (Fig. 3C). This may be related to the dynamic equilibrium between the generation of upstream autophagy-related molecules and the clearance of downstream molecules. Furthermore, as shown in Fig. 3D, reciprocal co-IP revealed an interaction between P62, the adapter protein in autophagosomes, and PLIN2, the pre-

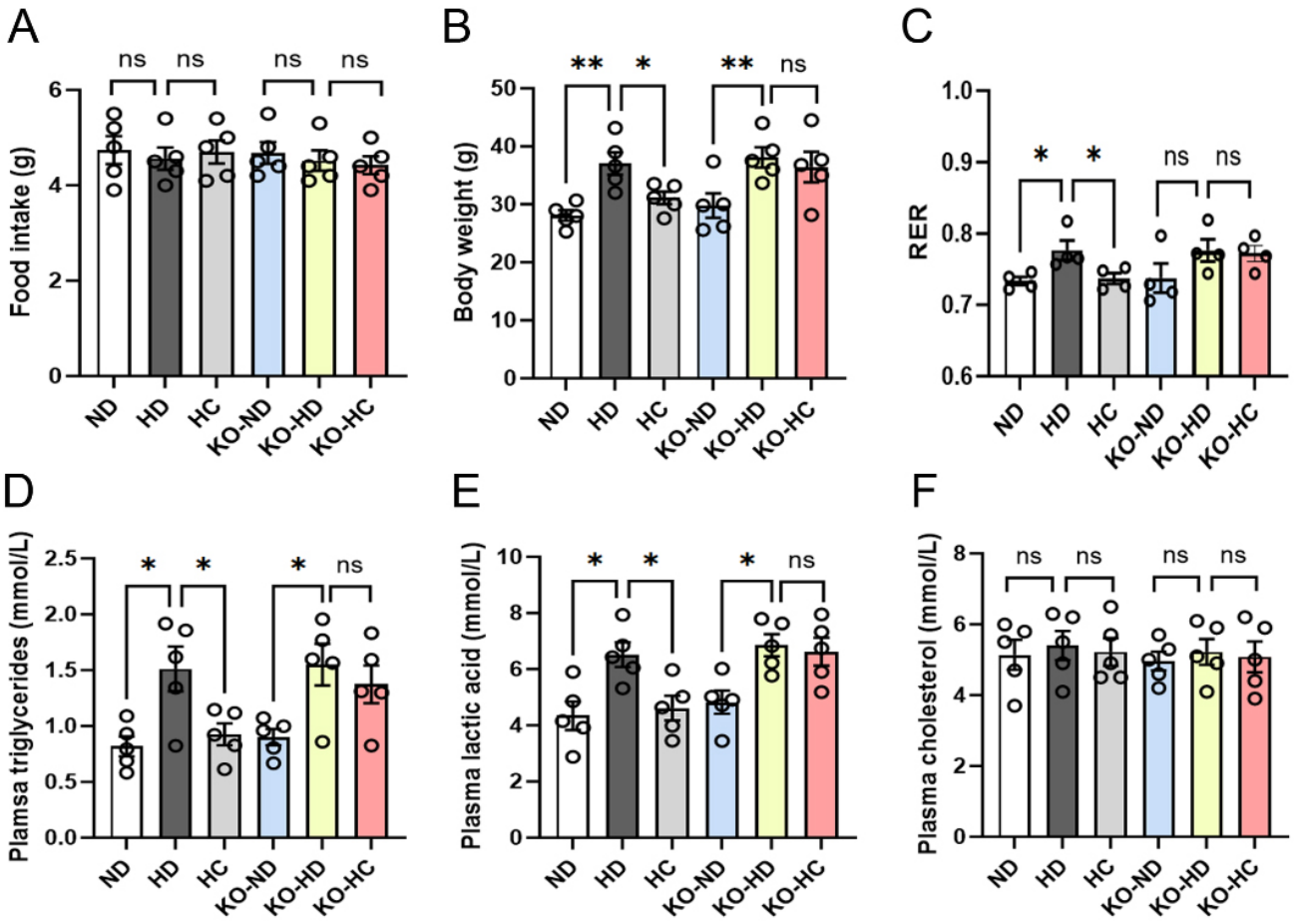

Fig. 1. Metabolic parameters of wild-type and *TRPV1* gene knock-out (KO) mice with chow (normal diet, ND), high-fat diet (HD), and high-fat plus 0.01% capsaicin diet (HC) for 4 months. (A) Daily food intake. (B) Body weight. (C) Respiratory exchange ratio (RER). (D) Plasma triglycerides. (E) Plasma lactic acid. (F) Plasma cholesterol. N = 4 or 5. Data are shown as mean ± standard error of the means (SEM). *, $p < 0.05$; **, $p < 0.01$; ns, not significant.

dominant lipid droplet coating protein in muscles (Fig. 3D). Finally, the ultrastructure of muscle fibers was observed by electron microscopy (Fig. 3E). Mitochondrial swelling with visible vacuoles was shown in mice with HD, but relieved in mice with HD supplemented with capsaicin. However, autophagosomes containing lipid droplets were not observed or were difficult to distinguish in the muscle fibers.

Capsaicin Restores the Palmitate-Induced Impairment of Autophagy Flux and Lipid Utilization in C2C12 Myotubes via TRPV1 Activation

To further elucidate the mechanisms, C2C12 myoblasts were incubated and differentiated into myotubes *in vitro*. As saturated fatty acids in most diets are primarily represented by palmitic acid [28], we incubated C2C12 myotubes with palmitate (0.5 mM) combined with BSA for 20 hours to induce lipid accumulation and insulin resistance as described previously [22,25]. The palmitate-treated myotubes were also stimulated with or without the autophagy inhibitor chloroquine or different concentrations of capsaicin. Oil-red O staining showed that palmitate incubation led to increased intracellular lipid droplets (LDs) compared to the control group ($p < 0.05$). Capsaicin dose-dependently decreased the palmitate-induced LDs, with a maximum reduction at the concentration of 10 μM ($p < 0.05$). While chloroquine significantly exaggerated the lipid accumulation in myotubes ($p < 0.05$) (Fig. 4A,B).

To investigate how capsaicin affected lipid metabolism, we measured the fatty acid oxidation rate by 14C-palmitate tracing. The 14C-labeled CO_2 released from palmitate oxidation (representing complete fatty acid oxidation) and the remaining cell-associated (CA) radioactivity (representing intracellular unmetabolized palmitate and incomplete oxidation) were collected and counted. As shown in Fig. 4C, capsaicin promoted complete palmitate oxidation ($p < 0.05$). This increase was suppressed by the TRPV1 antagonist capsazepine ($p < 0.05$). Also, chloroquine markedly inhibited the complete oxidation of 14C-palmitate ($p < 0.05$). On the other hand, capsaicin significantly decreased the residual CA radioactivity, representing intracellular palmitate and its metabolic intermediates. The total uptake of

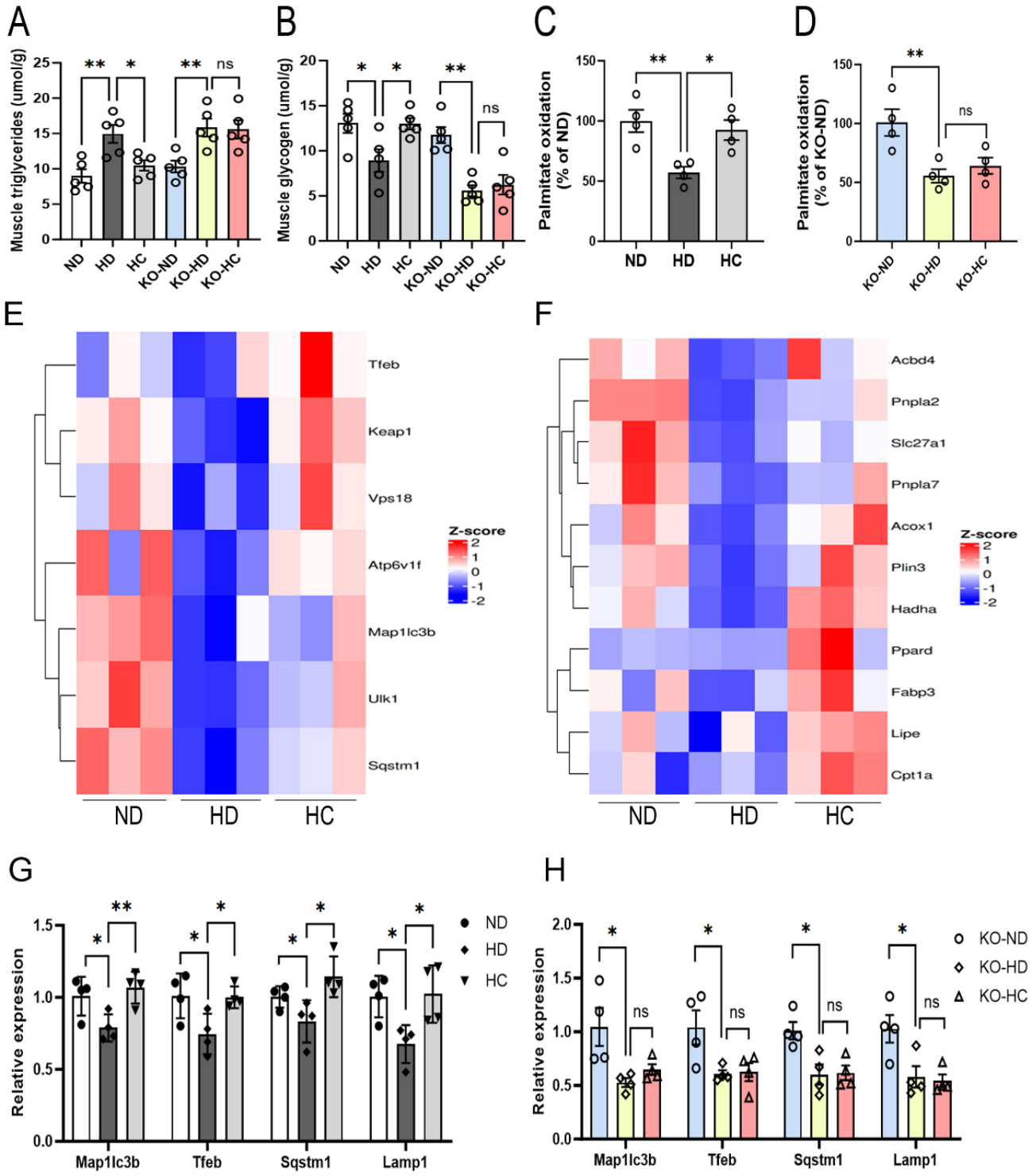

Fig. 2. Skeletal muscle triglyceride utilization and autophagy-related gene expression levels. (A,B) triglycerides (A) and glycogen (B) contents in gastrocnemius muscles. N = 5. (C,D) 14-C-palmitate oxidation in incubated mitochondria isolated from gastrocnemius muscles of wild-type (C) and *TRPV1* gene knock-out (D) mice after an aerobic exercise under fasted conditions. N = 4. (E,F) heat map illustrating RNA-Seq differential expression related to autophagy (E) and fatty acid oxidation (F) in soleus muscles of wild-type mice. Comparisons are shown for mice on a normal diet (ND) and high-fat plus capsaicin diet (HC) vs. high-fat diet (HD). Red, positive log fold-change (log FC) indicates higher expression. N = 3. (G,H) mRNA expression levels (by RT-qPCR) in wild-type (G) and *TRPV1* gene knockout (H) mice. N = 4. Data are shown as mean ± SEM. *, $p < 0.05$; **, $p < 0.01$; ns, not significant.

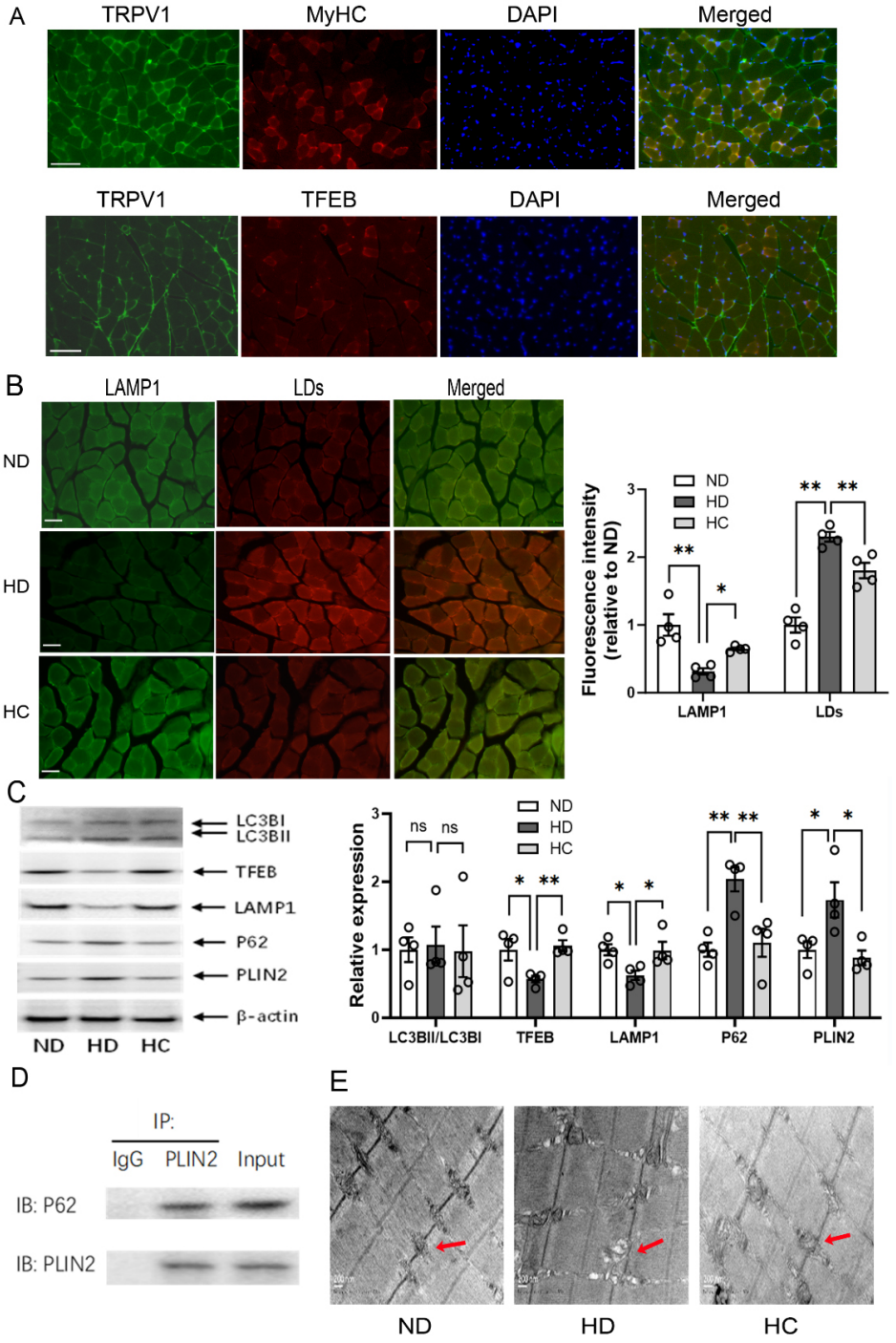

Fig. 3. Capsaicin attenuated the impaired autophagosomes and lipid clearance induced by the high-fat diet in wild-type mice. (A) Upper: Representative immunofluorescence images show TRPV1 (green) expressed on the membrane of all fiber types and within the cytoplasm of type I fibers labeled with anti MyHC (red). Lower: Representative immunofluorescence images demonstrate cytoplasmic co-localization of TRPV1 (green) and TFEB (red) in type I fibers, though TRPV1 expression remains more abundant on the cell membrane. The muscle fibers were from wild-type mice on a normal diet. The scale bar is 100 µm. (B) Immunofluorescence showing lipid droplets (LDs, stained by Nile red) and lysosomes (green, labeled by anti-LAMP1 antibody) in skeletal muscles. N = 4. The scale bar is 50 µm. *, $p < 0.05$; **, $p < 0.01$. (C) Protein expression levels related to autophagy and lipid droplet coating in muscles of wild-type mice by immunoblotting. N = 4. Data are shown as mean ± SEM. *, $p < 0.05$; **, $p < 0.01$; ns, not significant. (D) co-IP showing the combination of P62 and PLIN2. (E) Representative electron microscope images showing soleus muscles of mice. The scale bar is 200 nm. Red arrows indicate representative mitochondria. ND, normal diet; HD, high-fat diet; HC, high-fat plus capsaicin diet; MyHC, myosin heavy chain; LAMP1, lysosomal-associated membrane protein 1; co-IP, co-immunoprecipitation; PLIN2, Perilipin 2.

14C-palmitate, calculated as the sum of 14-labeled CO_2 and CA-radioactivity normalized to the protein content, was not affected by either capsaicin or chloroquine ($p > 0.05$) (Fig. 4C).

Then, we determined the autophagic flux by transducing the RFP-GFP-LC3B tan-dem sensor. Relative to the BSA-treated control group, autolysosomes (red puncta) in the palmitate-treated group were significantly reduced ($p < 0.05$), suggesting the palmitate-induced impairment in autophagosome-lysosome fusion. The palmitate-induced autolysosome reduction was significantly attenuated by capsaicin treatment ($p < 0.05$). This effect of capsaicin was partially blocked by the co-incubation of capsazepine ($p < 0.05$) (Fig. 4D,E). Cells of the above groups were also stained with the acidic pH-triggered lysosome marker to measure the content of functional lysosomes. It showed that capsaicin significantly restored the palmitate-induced reduction of acidic lysosomes ($p < 0.05$) (Fig. 4F,G). Representative autolysosomes containing debris were observed by transmission electron microscopy (TEM) in 3 groups of C2C12 cells (Fig. 4H). However, due to technical reasons, we were unfortunately unable to obtain electron micrographs for the group treated with the combination of capsaicin and capsazepine. These results indicate that capsaicin can effectively restore the acidic lysosome content, autophagy flux, and lipid oxidation in palmitate-treated C2C12 myotubes, effects that are largely dependent on TRPV1 activation.

Capsaicin Promotes TFEB Nuclear Translocation and Protein Expression Through TRPV1-Dependent Calcineurin Activation

TFEB acts as a master regulator of lysosome biogenesis and lipophagy [29,30]. TFEB undergoes dephosphorylation and translocates to the nucleus in response to the Ca^{2+} signaling, calcineurin [31]. Thus, we explored the effects of capsaicin on TFEB activity and expression. C2C12 myotubes were co-treated with capsaicin and either capsazepine or cyclosporine A (a calcineurin inhibitor) for 4 hours. Immunofluorescence staining showed remarkably increased nuclear localization of TFEB induced by capsaicin, which was blocked by the presence of either capsazepine or cyclosporine A (Fig. 5A). We detected the TFEB transcriptional activity using the dual-luciferase reporter system and found that the “CLEAR” activity in capsaicin-treated myotubes was also enhanced ($p < 0.05$) (Fig. 5B). It meant that capsaicin significantly enhanced the TFEB combining ability to the “CLEAR” DNA sequence in the regulatory region of lysosomal genes and induced their transcription. Capsaicin treatment also significantly increased the calcineurin activity in myotubes ($p < 0.05$), and this effect was remarkably abolished by the coexistence of cyclosporine A ($p < 0.05$), capsazepine ($p < 0.05$), or the calcium chelator EGTA ($p < 0.05$) (Fig. 5C). TFEB protein expression was further detected in myotubes incubated with increasing concentrations of capsaicin for 20 hours. It showed that capsaicin dose-dependently upregulated TFEB expression within a concentration range of 1 μM to 10 μM ($p < 0.05$) (Fig. 5D,E). On the other hand, although the TFEB expression was significantly downregulated by palmitate in myotubes ($p < 0.05$), it was restored by the addition of capsaicin ($p < 0.05$) (Fig. 5F,G). The effect of capsaicin on TFEB expression was also abolished by either capsazepine or cyclosporin A ($p < 0.05$) (Fig. 5F,G). These results indicate that capsaicin promotes the nuclear localization and the protein expression of TFEB via TRPV1/calcineurin signaling in C2C12 myotubes.

Capsaicin Attenuates the Palmitate-Induced Impairment of Lipophagy via TRPV1/Calcineurin/TFEB Activation

Microtubule-associated protein 1 light chain 3B (LC3B) and p62 serve as classic marker proteins for monitoring autophagy [2]. LC3BII, converted from LC3BI lipidation, is incorporated in autophagosomes. The adapter protein associates ubiquitinated proteins with LC3BII to promote their recycling. P62 and target proteins accumulate when the downstream autophagy flux is blocked [2]. The major LD-coating protein in skeletal muscle is Perilipin 2 (PLIN2), which normally protects triglycerides from turnover [32,33]. However, when lipophagy is enhanced, PLIN2 can bind to p62 and be degraded in L6 myotubes [7].

We further investigated the above lipophagy markers by immunoblotting. It showed that p62 and PLIN2 were both upregulated in palmitate-treated myotubes ($p < 0.05$), which were partially inhibited by the addition of capsaicin ($p < 0.05$). Whereas lysosomal-associated membrane protein 1 (LAMP1), the lysosomal marker, was downregulated in palmitate-treated myotubes ($p < 0.05$), which was restored by the addition of capsaicin ($p < 0.05$). The capsaicin-induced changes in these proteins were blocked by either capsazepine or cyclosporine A ($p < 0.05$) (Fig. 6A–C). However, the ratio of LC3B II/LC3B I was not affected by either palmitate or capsaicin ($p > 0.05$) (Fig. 6B), which might be due to the mixed effects on the rates of LC3B lipidation and clearance. Immunofluorescence assay showed that there were more LDs (stained with the LDs-specific fluorescent dye Nile Red) and less LAMP1 surrounding the LDs in palmitate-treated myotubes, while the addition of capsaicin attenuated the effect of palmitate (Fig. 6D,E).

To verify the involvement of TFEB in the aforementioned effects of capsaicin, we knocked down TFEB gene expression by more than 75% via TFEB siRNA transfection. The 14C-palmitate oxidation rate (Fig. 6F) was significantly inhibited and the protein level of p62 (Fig. 6G,H) was significantly increased by TFEB siRNA ($p < 0.05$). Capsaicin treatment could not reverse the effects of TFEB siRNA, as there was no difference between the two groups

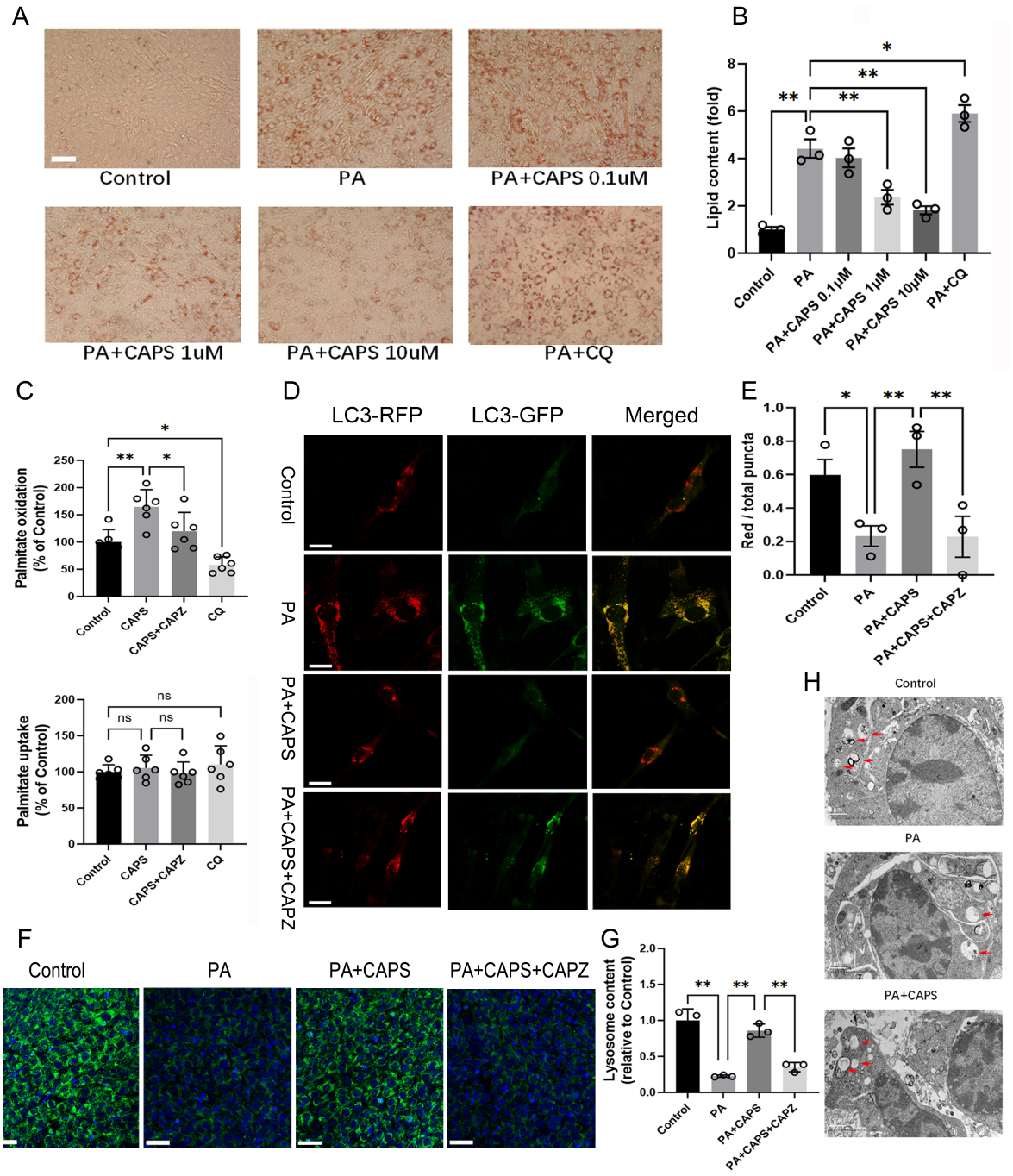

Fig. 4. Capsaicin restored the impaired autophagy flux and lipid utilization in C2C12 myotubes treated with palmitate, effects that are dependent on TRPV1. (A,B) Lipid contents in myotubes incubated with palmitate (PA) alone or combined with chloroquine (CQ, 50 μM) or different concentrations of capsaicin (CAPS) for 20 hours. Representative images by oil-red O (A) and bar charts of summary statistics (B) are shown. N = 3. The scale bar is 100 μm. (C) 14C-palmitate oxidation, and the total palmitate uptake of myotubes pre-treated with CQ or capsaicin (1 μM) in the presence or absence of capsazepine (CAPZ, 10 μM). N = 6. (D,E) Autophagy flux in C2C12 cells expressing RFP-GFP-LC3B treated with indicated combinations of PA, CAPS (1 μM), and CAPZ. Representative images (D) and bar charts of summary statistics (E) are shown. N = 3. The scale bar is 25 μm. (F,G) Acidic lysosome contents in myotubes. Representative images stained by LysoTracker Green DND-26 (F) and bar charts of summary statistics (G) are shown. The nuclei were stained by Horchest 33342. N = 3. The scale bar is 100 μm. (H) Representative electron microscope images showing the autolysosomes in myotubes treated with PA with or without CAPS. Red arrows: autolysosomes. The scale bar is 1 μm. *, $p < 0.05$; **, $p < 0.01$; ns, not significant.

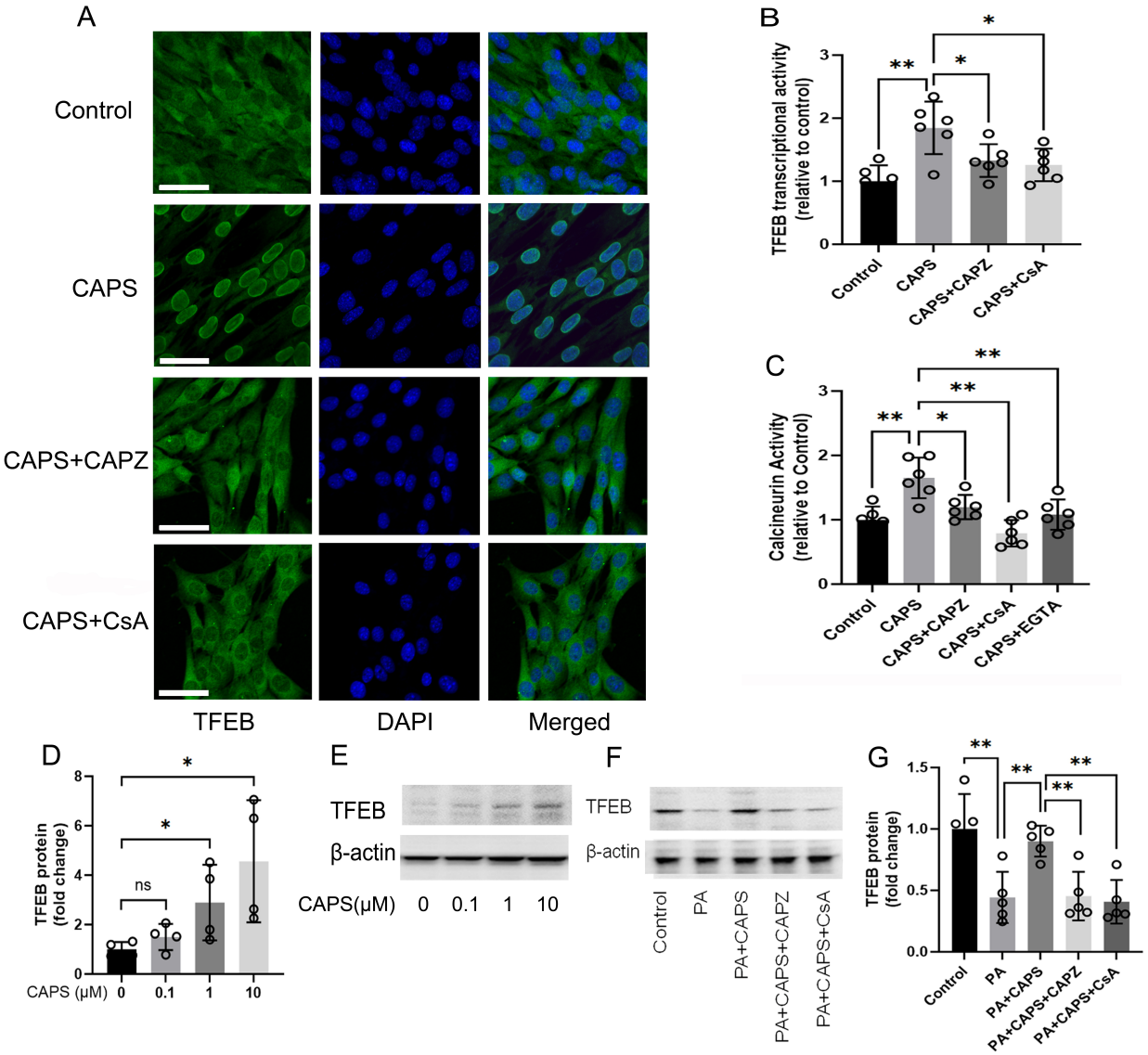

Fig. 5. Capsaicin promoted TFEB nuclear translocation and protein expression through TRPV1-dependent calcineurin activation in C2C12 myotubes. (A) Representative images showing TFEB (green) distribution in myotubes treated with capsaicin (CAPS) in the presence or absence of capsazepine (CAPZ) or cyclosporine A (CsA) for 4 hours. The scale bar is 100 μm. (B) TFEB transcriptional activity detected using the dual-luciferase reporter system. N = 6. (C) Calcineurin activity in myotubes treated with CAPS in the presence or absence of CAPZ, CsA, or calcium chelator EGTA for 4 hours. N = 6. (D,E) TFEB protein expression in myotubes treated with different concentrations of CAPS for 20 hours. Bar charts of summary statistics (D) and representative bands (E) are shown. N = 4. (F,G) TFEB protein level in myotubes treated with CAPS in the presence or absence of CAPZ or CsA for 20 hours. Representative bands (F) and bar charts of summary statistics (G) are shown. N = 5. *, $p < 0.05$; **, $p < 0.01$; ns, not significant.

with TFEB siRNA ($p > 0.05$) (Fig. 6F–H). These results indicate that TFEB was critical for the effect of capsaicin on lipophagy and fatty acid oxidation.

Discussion

Muscular lipid accumulation is a key factor in the development of insulin resistance and related metabolic diseases [1]. Our findings indicate that capsaicin-mediated TRPV1 activation promotes lipid oxidation and reduces intramuscular lipid deposition by regulating TFEB-mediated lipophagy flux.

Previous studies have demonstrated that dietary capsaicin consumption can lower serum triglyceride levels, promote fat oxidation in fat tissues, and reduce fat weight [11,12,34,35]. Skeletal muscle investigations in rodents showed that dietary capsaicin led to fast-to-slow muscle fiber conversion and upregulation of proteins related to lipid metabolism, including PGC1a and CD36, which might suggest a shift in fuel preference from glycolysis to fatty acid

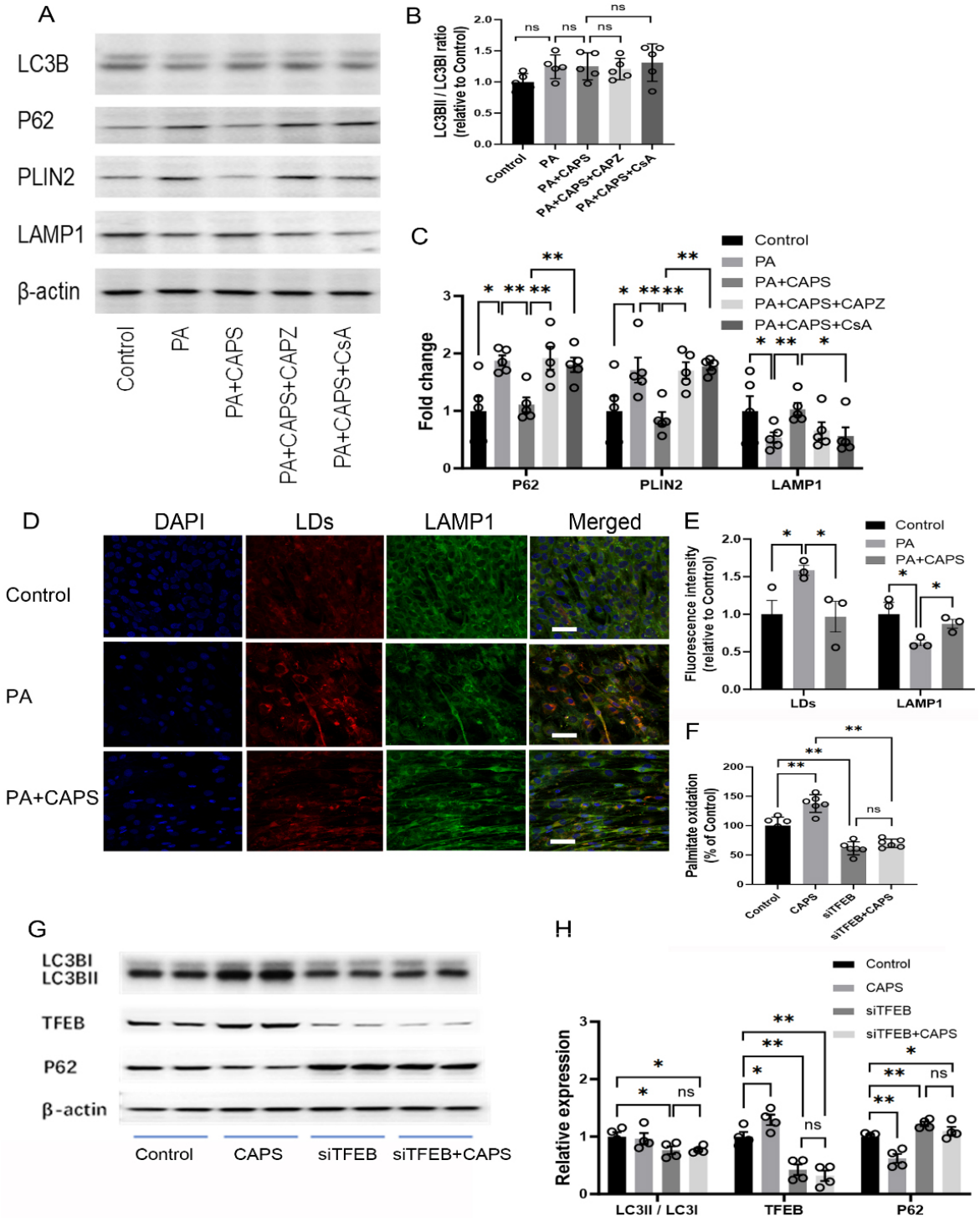

Fig. 6. Capsaicin attenuated the palmitate-induced impairment of lipid autophagy via TRPV1/calcineurin/TFEB activation. (A–C) The protein expression of PLIN2 and key autophagy genes in myotubes treated with palmitate (PA), capsaicin (CAPS) in the absence or presence of capsazepine (CAPZ) or cyclosporine A (CsA) for 20 hours. Representative bands (A) and bar charts of summary statistics (B,C) are shown. N = 5. *, $p < 0.05$; **, $p < 0.01$; ns, not significant. (D) Representative immunofluorescence images showing Nile red-stained lipid droplets (LDs, red) and LAMP1 (green) in myotubes treated with PA alone or together with CAPS. The scale bar is 100 μm. (E) The summary statistics of the fluorescence intensity of LDs and LAMP1. N = 3. *, $p < 0.05$. (F–H) 14C-palmitate oxidation rate (F) and the protein expression of key autophagy genes in C2C12 cells with scrambled siRNA transfection (Control) or TFEB RNA interference (siTFEB) in the absence or presence of capsaicin (CAPS). Representative bands (G) and bar charts of summary statistics (H) are shown. N = 4. *, $p < 0.05$; **, $p < 0.01$; ns, not significant.

oxidation [17,36]. The capsaicin-induced fatty acid oxidation *in vivo* was confirmed in the present study on the skeletal muscles of mice and cultured myotubes. However, capsaicin exhibits no significant effect on fatty acid uptake *in vitro*, which was inconsistent with the upregulated CD36 in muscles from rodents with dietary capsaicin [36]. It might be partially due to the differences in extracellular conditions, including fatty acid availability, between *in vitro* and *in vivo* studies. Our findings also showed reduced residual intracellular fatty acid and the related intermediates produced by incomplete oxidation in capsaicin-treated myotubes, which might contribute to the attenuation of insulin resistance induced by toxic lipid intermediates.

Autophagic activity is intricately linked to lipid metabolism. On the one hand, through lipophagy, LDs are targeted for sequestration by autophagosomes and degradation by lysosomes. On the other hand, chronic palmitate treatment leads to lysosome dysfunction and impaired autophagy flux [37,38], which partially contributes to lipotoxicity. Autophagy inhibitor treatment can accelerate lipid accumulation in cultured L6 myotubes [7]. Similar findings were observed in our study on mice fed with HD and by treating C2C12 myotubes with palmitate and chloroquine.

Most importantly, our study discovered that capsaicin restored the palmitate-induced impairment of lipophagy flux in myotubes through a TRPV1/calcineurin/TFEB pathway, suggesting that capsaicin can act as a lipophagy enhancer in myotubes. Basak *et al*. [39] recently reported that capsaicin inhibited Shigella flexneri growth by inducing autophagy in rodent macrophages and intestinal cells. Capsaicin (16 μM) treatment for 2 hours increased the nuclear localization of TFEB, which further induced autophagosomal gene transcription [39]. Accordingly, our study showed that in C2C12 myotubes, capsaicin (1 μM) treatment not only increased the TFEB nuclear localization in 4 hours but also upregulated TFEB protein expression in 24 hours.

Furthermore, it has been reported that calcineurin, an endogenous serine/threonine phosphatase, can be activated by calcium signaling and dephosphorylate TFEB, leading to autophagy enhancement [31]. Here, we found that calcineurin activity was enhanced by capsaicin through TRPV1-dependent calcium signaling, which contributed to the TFEB activation in myotubes. Zhou G *et al*. [36] showed that the protein expression of calcineurin was upregulated in the skeletal muscles of rats with long-term dietary capsaicin intake. Calcineurin activity was also shown to be activated by TRPV1-mediated calcium signals in human keratinocytes [40]. Hurt CM *et al*. [41] identified an interaction site for TRPV1 with calcineurin in the mitochondria of cardiomyocytes using in silico analysis and rodent experiments, and that the combining activity of TRPV1 to calcineurin could be modulated by a synthetic peptide. These studies are partially consistent with our findings in capsaicin-treated myotubes. However, whether TRPV1 can directly bind to calcineurin in myotubes and whether TRPV1 channels at subcellular organelles have different functions in myotubes warrant further exploration.

The present study identified LDs as the target of capsaicin-induced autophagy by the co-immunoprecipitation of p62 and PLIN2 and the co-localization of LDs and lysosome marker LAMP1. Recent evidence reveals that p62 links perilipin-coated LDs to phagophores via its scaffold function [42], ultimately targeting both for co-degradation in lysosomes [43]. Our study suggests that p62 and PLIN2-marked LDs accumulate in myotubes treated with a high concentration of palmitate, which is associated with impaired TFEB expression and lysosome function, and this pathological state can be attenuated by capsaicin-induced TRPV1/TFEB activation. Wang *et al*. [44] demonstrated that TFEB upregulation improves palmitate-induced insulin resistance in C2C12 myotubes by enhancing autophagy and AMPK activity. This aligns with TFEB's broader roles in regulating diverse processes, including autophagic pathways, PGC1α expression, and mitochondrial biogenesis [19,29]. Chronic dietary capsaicin intake has been shown to increase PGC1α expression and mitochondrial content in mouse skeletal muscles [17]. Thus, the enhanced fatty acid oxidation induced by capsaicin is underpinned by both increased lipophagy and improved mitochondrial function.

Several limitations of this study should be acknowledged. First, because the experiments were performed exclusively in male mice, the outcomes might not be generalizable to female mice or other species. Second, although multiple approaches were employed to test the hypotheses, the quality of the electron microscopy images was insufficient to clearly resolve subcellular details. Third, while the present study suggests differential distributions of TRPV1 and TFEB across distinct muscle fiber types, the implications of these differences were not explored in depth. Future studies applying more advanced techniques, such as single-cell sequencing, may help to clarify the underlying mechanisms. Finally, although our data indicate calcineurin in capsaicininduced TFEB activation, the precise mechanistic role of this pathway remains to be fully elucidated.

Conclusions

Capsaicin restores the deficiency in lipophagy and fatty acid oxidation in lipid-overloaded myotubes through a TRPV1/calcineurin/TFEB pathway. The findings provide new insights into the role of TRPV1 in myotubes and may contribute to the development of alternative approaches to prevent lipotoxicity and metabolic diseases.

Availability of Data and Materials

The main data are contained within the article and the **Supplementary Materials**. The raw RNA-sequencing data have been uploaded to the NCBI database (PRJNA1290807).

Author Contributions

LW and YZ performed the experiments, analyzed the data, and prepared the original draft. SW, LL, YH, and YC provided technical support, performed experiments and contributed to drafting the initial manuscript. ZL designed the research, interpreted the data, and critically revised the manuscript. ZL provided financial support. All authors gave final approval of the version to be published. All authors have participated sufficiently in the work to take public responsibility for appropriate portions of the content and agreed to be accountable for all aspects of the work in ensuring that questions related to its accuracy or integrity.

Ethics Approval and Consent to Participate

All mice were cared for and used in the study in compliance with international, national, and institutional guidelines, following approval from the Chongqing General Hospital Animal Care and Research Advisory Committee. Ethical approval for the study protocol was obtained on March 15, 2017.

Acknowledgment

Not applicable.

Funding

This work was supported by grants from the National Natural Science Foundation of China (No. 81770801) and the Discipline Talent Program of Chongqing General Hospital (No. 2023122602).

Conflict of Interest

The authors declare no conflict of interest.

Supplementary Material

Supplementary material associated with this article can be found, in the online version, at https://doi.org/10.24976/Discov.Med.202638205.42.

References

[1] Gilbert M. Role of skeletal muscle lipids in the pathogenesis of insulin resistance of obesity and type 2 diabetes. Journal of Diabetes Investigation. 2021; 12: 1934–1941. https://doi.org/10.1111/jdi.13614.

[2] Filali-Mouncef Y, Hunter C, Roccio F, Zagkou S, Dupont N, Primard C, *et al*. The ménage à trois of autophagy, lipid droplets and liver disease. Autophagy. 2022; 18: 50–72. https://doi.org/10.1080/15548627.2021.1895658.

[3] Nakamura J, Yamamoto T, Takabatake Y, Namba-Hamano T, Minami S, Takahashi A, *et al*. TFEB-mediated lysosomal exocytosis alleviates high-fat diet-induced lipotoxicity in the kidney. JCI Insight. 2023; 8: e162498. https://doi.org/10.1172/jci.insight.162498.

[4] van Niekerk G, du Toit A, Loos B, Engelbrecht AM. Nutrient excess and autophagic deficiency: explaining metabolic diseases in obesity. Metabolism: Clinical and Experimental. 2018; 82: 14–21. https://doi.org/10.1016/j.metabol.2017.12.007.

[5] Yang L, Li P, Fu S, Calay ES, Hotamisligil GS. Defective hepatic autophagy in obesity promotes ER stress and causes insulin resistance. Cell Metabolism. 2010; 11: 467–478. https://doi.org/10.1016/j.cmet.2010.04.005.

[6] Kim J, Kim SH, Kang H, Lee S, Park SY, Cho Y, *et al*. TFEB-GDF15 axis protects against obesity and insulin resistance as a lysosomal stress response. Nature Metabolism. 2021; 3: 410–427. https://doi.org/10.1038/s42255-021-00368-w.

[7] Lam T, Harmancey R, Vasquez H, Gilbert B, Patel N, Hariharan V, *et al*. Reversal of intramyocellular lipid accumulation by lipophagy and a p62-mediated pathway. Cell Death Discovery. 2016; 2: 16061. https://doi.org/10.1038/cddiscovery.2016.61.

[8] Christie S, Wittert GA, Li H, Page AJ. Involvement of TRPV1 Channels in Energy Homeostasis. Frontiers in Endocrinology. 2018; 9: 420. https://doi.org/10.3389/fendo.2018.00420.

[9] Panchal SK, Bliss E, Brown L. Capsaicin in Metabolic Syndrome. Nutrients. 2018; 10: 630. https://doi.org/10.3390/nu10050630.

[10] Sun F, Xiong S, Zhu Z. Dietary Capsaicin Protects Cardiometabolic Organs from Dysfunction. Nutrients. 2016; 8: 174. https://doi.org/10.3390/nu8050174.

[11] Wu Y, Liu W, Wang R, Lian Y, Cheng X, Yang R, *et al*. Capsaicin and Quercitrin Maintained Lipid Homeostasis of Hyperlipidemic Mice: Serum Metabolomics and Signaling Pathways. Foods (Basel, Switzerland). 2024; 13: 3727. https://doi.org/10.3390/foods13233727.

[12] Zheng J, Zheng S, Feng Q, Zhang Q, Xiao X. Dietary capsaicin and its anti-obesity potency: from mechanism to clinical implications. Bioscience Reports. 2017; 37: BSR20170286. https://doi.org/10.1042/BSR20170286.

[13] Yang Q, La C, Prabahar K, Safargar M, Kord-Varkaneh H, Temuqile, *et al*. The effect of capsaicin, capsinoids, and pepper-based interventions on lipid profiles in overweight or obese individuals: a systematic review and meta-analysis of randomized controlled trials. Diabetes Research and Clinical Practice. 2025; 229: 112478. https://doi.org/10.1016/j.diabres.2025.112478.

[14] Ávila DL, Fernandes-Braga W, Silva JL, Santos EA, Campos G, Leocádio PCL, *et al*. Capsaicin Improves Systemic Inflammation, Atherosclerosis, and Macrophage-Derived Foam Cells by Stimulating PPAR Gamma and TRPV1 Receptors. Nutrients. 2024; 16: 3167. https://doi.org/10.3390/nu16183167.

[15] Song H, Xie M, Xu H, Liu J, Su A, Liu Y, *et al*. Capsaicin regulated lipid metabolism in HepG2 via mitochondrial autophagy PINK1/Parkin pathway. Gene. 2025; 968: 149752. https://doi.org/10.1016/j.gene.2025.149752.

[16] Yu H, Chen J, Wang F, Jia D, Bi S, Mao Y, *et al*. Capsaicin Alleviates Autophagy-Lysosomal Dysfunction via PPARA-Mediated V-ATPase Subunit ATP6V0E1 Signaling in 3xTg-AD Mice. Advanced Science (Weinheim, Baden-Wurttemberg, Germany). 2025; 12: e02707. https://doi.org/10.1002/advs.202502707.

[17] Luo Z, Ma L, Zhao Z, He H, Yang D, Feng X, *et al*. TRPV1 activation improves exercise endurance and energy metabolism through PGC-1α upregulation in mice. Cell Research. 2012; 22: 551–564. https://doi.org/10.1038/cr.2011.205.

[18] Skagen C, Løvsletten NG, Asoawe L, Al-Karbawi Z, Rustan AC, Thoresen GH, *et al*. Functional expression of the thermally activated transient receptor potential channels TRPA1 and TRPM8 in human myotubes. Journal of Thermal Biology. 2023; 116: 103623. https://doi.org/10.1016/j.jtherbio.2023.103623.

[19] Huang KC, Chiang YF, Huang TC, Chen HY, Lin PH, Ali M, *et al*. Capsaicin alleviates cisplatin-induced muscle loss and at-

rophy in vitro and in vivo. Journal of Cachexia, Sarcopenia and Muscle. 2023; 14: 182–197. https://doi.org/10.1002/jcsm.13120.

[20] Sukan-Karaçağıl B, Akbulut G, Açar Y, Demirkoparan M. A Little Pepper-Upper? Systematic Review of Randomized Controlled Studies on Capsaicinoids, Capsinoids, and Exercise Performance. International Journal of Sport Nutrition and Exercise Metabolism. 2023; 33: 291–301. https://doi.org/10.1123/ijsnem.2023-0016.

[21] Abdillah AM, Lee JY, Lee YR, Yun JW. Modulatory roles of capsaicin on thermogenesis in C2C12 myoblasts and the skeletal muscle of mice. Chemico-biological Interactions. 2025; 407: 111380. https://doi.org/10.1016/j.cbi.2025.111380.

[22] Li Q, Li L, Wang F, Chen J, Zhao Y, Wang P, *et al*. Dietary capsaicin prevents nonalcoholic fatty liver disease through transient receptor potential vanilloid 1-mediated peroxisome proliferator-activated receptor δ activation. Pflugers Archiv: European Journal of Physiology. 2013; 465: 1303–1316. https://doi.org/10.1007/s00424-013-1274-4.

[23] Hirotani Y, Fukamachi J, Ueyama R, Urashima Y, Ikeda K. Effects of Capsaicin Coadministered with Eicosapentaenoic Acid on Obesity-Related Dysregulation in High-Fat-Fed Mice. Biological & Pharmaceutical Bulletin. 2017; 40: 1581–1585. https://doi.org/10.1248/bpb.b17-00247.

[24] Li L, Ma L, Luo Z, Wei X, Zhao Y, Zhou C, *et al*. Lack of TRPV1 aggravates obesity-associated hypertension through the disturbance of mitochondrial Ca2+ homeostasis in brown adipose tissue. Hypertension Research: Official Journal of the Japanese Society of Hypertension. 2022; 45: 789–801. https://doi.org/10.1038/s41440-021-00842-8.

[25] Yudhani RD, Sari Y, Nugrahaningsih DAA, Sholikhah EN, Rochmanti M, Purba AKR, *et al*. *In Vitro* Insulin Resistance Model: A Recent Update. Journal of Obesity. 2023; 2023: 1964732. https://doi.org/10.1155/2023/1964732.

[26] Lund J, Aas V, Tingstad RH, Van Hees A, Nikolić N. Utilization of lactic acid in human myotubes and interplay with glucose and fatty acid metabolism. Scientific Reports. 2018; 8: 9814. https://doi.org/10.1038/s41598-018-28249-5.

[27] Wensaas AJ, Rustan AC, Lövstedt K, Kull B, Wikström S, Drevon CA, *et al*. Cell-based multiwell assays for the detection of substrate accumulation and oxidation. Journal of Lipid Research. 2007; 48: 961–967. https://doi.org/10.1194/jlr.D600047-JLR200.

[28] Carta G, Murru E, Banni S, Manca C. Palmitic Acid: Physiological Role, Metabolism and Nutritional Implications. Frontiers in Physiology. 2017; 8: 902. https://doi.org/10.3389/fphys.2017.00902.

[29] Settembre C, De Cegli R, Mansueto G, Saha PK, Vetrini F, Visvikis O, *et al*. TFEB controls cellular lipid metabolism through a starvation-induced autoregulatory loop. Nature Cell Biology. 2013; 15: 647–658. https://doi.org/10.1038/ncb2718.

[30] Settembre C, Zoncu R, Medina DL, Vetrini F, Erdin S, Erdin S, *et al*. A lysosome-to-nucleus signalling mechanism senses and regulates the lysosome via mTOR and TFEB. The EMBO Journal. 2012; 31: 1095–1108. https://doi.org/10.1038/emboj.2012.32.

[31] Tong Y, Song F. Intracellular calcium signaling regulates autophagy via calcineurin-mediated TFEB dephosphorylation. Autophagy. 2015; 11: 1192–1195. https://doi.org/10.1080/15548627.2015.1054594.

[32] Feng YZ, Lund J, Li Y, Knabenes IK, Bakke SS, Kase ET, *et al*. Loss of perilipin 2 in cultured myotubes enhances lipolysis and redirects the metabolic energy balance from glucose oxidation towards fatty acid oxidation. Journal of Lipid Research. 2017; 58: 2147–2161. https://doi.org/10.1194/jlr.M079764.

[33] Tsai TH, Chen E, Li L, Saha P, Lee HJ, Huang LS, *et al*. The constitutive lipid droplet protein PLIN2 regulates autophagy in liver. Autophagy. 2017; 13: 1130–1144. https://doi.org/10.1080/15548627.2017.1319544.

[34] Yang J, Li W, Wang Y. Capsaicin Reduces Obesity by Reducing Chronic Low-Grade Inflammation. International Journal of Molecular Sciences. 2024; 25: 8979. https://doi.org/10.3390/ijms25168979.

[35] Zhang LL, Yan Liu D, Ma LQ, Luo ZD, Cao TB, Zhong J, *et al*. Activation of transient receptor potential vanilloid type-1 channel prevents adipogenesis and obesity. Circulation Research. 2007; 100: 1063–1070. https://doi.org/10.1161/01.RES.0000262653.84850.8b.

[36] Zhou G, Wang L, Xu Y, Yang K, Luo L, Wang L, *et al*. Diversity effect of capsaicin on different types of skeletal muscle. Molecular and Cellular Biochemistry. 2018; 443: 11–23. https://doi.org/10.1007/s11010-017-3206-7.

[37] Choi JW, Ohn JH, Jung HS, Park YJ, Jang HC, Chung SS, *et al*. Carnitine induces autophagy and restores high-fat diet-induced mitochondrial dysfunction. Metabolism: Clinical and Experimental. 2018; 78: 43–51. https://doi.org/10.1016/j.metabol.2017.09.005.

[38] Yamamoto T, Takabatake Y, Takahashi A, Kimura T, Namba T, Matsuda J, *et al*. High-Fat Diet-Induced Lysosomal Dysfunction and Impaired Autophagic Flux Contribute to Lipotoxicity in the Kidney. Journal of the American Society of Nephrology: JASN. 2017; 28: 1534–1551. https://doi.org/10.1681/ASN.2016070731.

[39] Basak P, Maitra P, Khan U, Saha K, Bhattacharya SS, Dutta M, *et al*. Capsaicin Inhibits *Shigella flexneri* Intracellular Growth by Inducing Autophagy. Frontiers in Pharmacology. 2022; 13: 903438. https://doi.org/10.3389/fphar.2022.903438.

[40] Kusumaningrum N, Lee DH, Yoon HS, Park CH, Chung JH. Ultraviolet light-induced gasdermin C expression is mediated via TRPV1/calcium/calcineurin/NFATc1 signaling. International Journal of Molecular Medicine. 2018; 42: 2859–2866. https://doi.org/10.3892/ijmm.2018.3839.

[41] Hurt CM, Lu Y, Stary CM, Piplani H, Small BA, Urban TJ, *et al*. Transient Receptor Potential Vanilloid 1 Regulates Mitochondrial Membrane Potential and Myocardial Reperfusion Injury. Journal of the American Heart Association. 2016; 5: e003774. https://doi.org/10.1161/JAHA.116.003774.

[42] Kageyama S, Gudmundsson SR, Sou YS, Ichimura Y, Tamura N, Kazuno S, *et al*. p62/SQSTM1-droplet serves as a platform for autophagosome formation and anti-oxidative stress response. Nature Communications. 2021; 12: 16. https://doi.org/10.1038/s41467-020-20185-1.

[43] Shroff A, Nazarko TY. SQSTM1, lipid droplets and current state of their lipophagy affairs. Autophagy. 2023; 19: 720–723. https://doi.org/10.1080/15548627.2022.2094606.

[44] Wang P, Li CG, Zhou X, Ding S. Transcription factor EB enhances autophagy and ameliorates palmitate-induced insulin resistance at least partly via upregulating AMPK activity in skeletal muscle cells. Clinical and Experimental Pharmacology & Physiology. 2022; 49: 302–310. https://doi.org/10.1111/1440-1681.13600.